

Quantum Electrodynamics Coupled-Cluster Theory: Exploring Photon-Induced Electron Correlations

Himadri Pathak,^{1,*} Nicholas P. Bauman,² Ajay Panyala,¹ and Karol Kowalski^{2,†}

¹*Advanced Computing, Mathematics, and Data Division,*

Pacific Northwest National Laboratory, Richland, Washington 99354, United States

²*Physical Sciences Division, Pacific Northwest National Laboratory, Richland, Washington 99354, United States*

(Dated: September 12, 2024)

We present our successful implementation of the quantum electrodynamics coupled-cluster method with single and double excitations (QED-CCSD) for electronic and bosonic amplitudes, covering both individual and mixed excitation processes within the ExaChem program package, which relies on the Tensor Algebra for Many-body Methods (TAMM) infrastructure. TAMM is a parallel heterogeneous tensor library designed for utilizing modern computing platforms, from laptops to leadership-class computing resources. This developed computational framework extends the traditional CCSD method to incorporate the intricate interplay between electronic and bosonic degrees of freedom, providing a comprehensive description of quantum phenomena. We discuss theoretical foundations, algorithmic details, and numerical benchmarks to demonstrate how the integration of bosonic degrees of freedom alters the electronic ground state. The interactions between electrons and photons within an optical cavity are modeled using the Pauli-Fierz Hamiltonian within the dipole approximation in the length gauge. The integration of QED effects within the CCSD framework contributes to a more accurate and versatile model for simulating complex quantum systems, thereby opening avenues for a better understanding, prediction, and manipulation of various physical phenomena.

I. INTRODCUTION

The quest for precise and comprehensive quantum mechanical models to describe complex systems has catalyzed the evolution of sophisticated methodologies within computational chemistry and quantum physics [1–4]. Advancements in high-performance computing now enable large-scale applications of these highly accurate techniques beyond model chemical systems [5, 6].

Polariton chemistry has emerged as a captivating field due to its potential to alter chemical structures, properties, and reactivity through profound interactions among molecular electronic, vibrational, and rovibrational states [7–14]. While several research groups within the quantum optics community have devised model Hamiltonians to encapsulate the core aspects of polaritonic physics [15–20], a holistic quantitative theoretical understanding of molecular polaritons demands the equal treatment of both matter and photon interactions with quantum mechanical precision. In scenarios where molecular electronic interactions are strongly or ultrastrongly coupled to one or a few molecules, the application of *ab initio* quantum chemistry techniques proves beneficial. This innovative approach, known as *ab initio* cavity quantum electrodynamics, seamlessly integrates the molecular electronic degrees of freedom with the principles of cavity quantum electrodynamics governing photon behavior. The emergence and refinement of various *ab initio* cavity quantum electrodynamics methodologies have gained significant traction in recent times.

Currently, the landscape of quantum electrodynamics extensions to various electronic structure methods includes density functional theory (QEDFT [21–27] and QED-DFT [28–30]), real-time [22, 23, 31–34] and linear-response formulations [28, 35, 36] of QED time-dependent density functional theory (QED-TDDFT), configuration interaction (QED-CIS) [37], cavity QED extensions of second-order Møller-Plesset perturbation theory, algebraic diagrammatic construction [38, 39], variational QED-2-RDM methods [40], and diffusion Monte Carlo [41]. Notably, the first formulation of QED-CASCI, both in the photon-number basis and the coherent-state basis, has recently been introduced [42].

The time-independent coupled-cluster (CC) method, along with its myriad extensions [43–52], has proven invaluable in addressing electron correlation across a spectrum of problems spanning both ground and excited states. The ground-state CC method exhibits size-extensivity across all levels of excitation operator truncation and scales polynomially with the number of active orbitals. These attributes render CC methods particularly attractive compared to alternative electron correlation techniques, striking a harmonious balance between computational efficiency and accuracy. Furthermore, the results can be systematically improved by encompassing more correlated determinantal spaces. A hallmark feature of CC methods lies in their use of an exponential parameterization for the correlated ground-state wavefunction $|\Psi\rangle: |\Psi\rangle = e^T |\Phi\rangle$, where T denotes the cluster operator and $|\Phi\rangle$ is a reference wavefunction, typically—but not exclusively—a Hartree-Fock wavefunction.

Two generalizations of coupled-cluster (CC) theory for incorporating quantum electrodynamics (QED) effects emerged around the same time. Mordovina *et al.* [54]

* himadri.pathak@pnnl.gov

† karol.kowalski@pnnl.gov

TABLE I: Comparison of QED-HF ground state energy and the correlation energy calculated at the CCSD(2, 2) level for the water molecule using various basis sets. Calculations were performed with the experimental geometry, with λ_z set to 0.1 and Ω_{cav} set to 3.0 eV.

Basis	QED-HF		CCSD(2, 2)	
	this work	Ref. [53]	this work	Ref. [53]
cc-pVDZ	-76.007 2646	-76.007 2646	-0.216 6871	-0.216 6871
aug-cc-pVDZ	-76.020 3868	-76.020 3868	-0.233 9280	-0.233 9280
cc-pVTZ	-76.036 8309	-76.036 8309	-0.285 2382	-0.285 2382
aug-cc-pVTZ	-76.039 6515	-76.039 6515	-0.292 9503	...

TABLE II: Comparison of total energies (in Hartree) for the H_2 molecule across various basis sets using an experimental bond length of 0.74 Å with $\lambda_z = 0.05$ and $\Omega_{cav} = 20.0$ eV. The molecule is oriented in the z -direction with one of the hydrogens placed at the (0, 0, 0) coordinate so that there is a non-zero dipole moment in the direction of polarization.

Basis	QED-CCSD(2,2)	QED-FCI [42]
cc-pVDZ	-1.162 4643	-1.162 4643
aug-cc-pVDZ	-1.163 6756	-1.163 6756
cc-pVTZ	-1.171 3895	-1.171 3895
aug-cc-pVTZ	-1.171 7020	...

introduced the polaritonic coupled-cluster theory, which used an exponential parameterization of the ground-state polaritonic wavefunction. This parameterization included single and double electronic transition operators, photon creation operators, and combined electron transition and photon creation operators. They applied this method, along with QED full configuration interaction (CI), to study strong coupling between a single photon mode and a four-site Hubbard model. Notably, they used nilpotent operators instead of conventional boson creation operators, resulting in a linear parameterization of the photon space. In contrast, the QED-CCSD-1 model by Haugland *et al.* [55] adopted a similarly complex exponential parameterization but used conventional (non-nilpotent) boson creation operators. They applied this model to address strong coupling in an ab initio molecular Hamiltonian.

Several research teams have developed and applied similar QED-CC approaches to study the impact of cavity effects on various ground-state properties. De-Prince [56] used QED-CCSD-1 to show how strong coupling alters electron affinities in sodium halide compounds significantly. However, cavity effects had less influence on ionization potentials in these systems.

Pavošević and Flick [57] went further into cavity interactions' effects on electron affinities by employing a unitary formulation of QED-CCSD-1. They used the variational quantum eigensolver (VQE) algorithm [58] on a

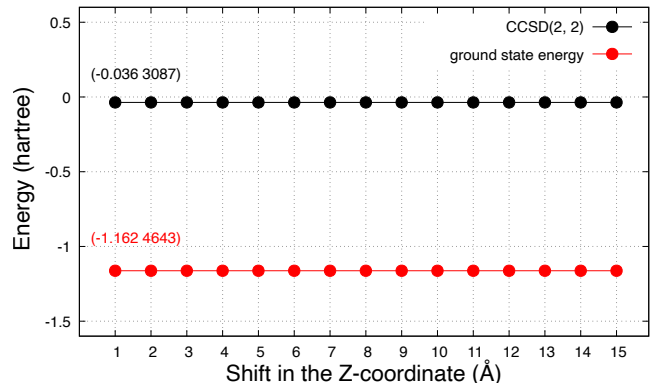


FIG. 1: Correlation energy computed at the CCSD(2, 2) level and total ground-state energy as a function of the shift in the Z -coordinate, with the SCF energy being -1.1261 556, which is also origin-invariant. The computations were performed with a shift in the Z -coordinate for the H_2 molecule using the aug-cc-pVDZ basis set. The calculations were carried out with $\lambda_z = 0.05$ and $\Omega_{cav} = 20.0$ eV. The molecule is oriented along the z -axis, with one hydrogen positioned at the (0, 0, 0) coordinate, resulting in a non-zero dipole moment aligned with the polarization direction.

quantum computer for this purpose. Additionally, they expanded the framework to include up to two photon creation operators, alongside single and double electronic excitations, which they called QED-CCSD-2.

These foundational studies paved the way for further exploration of ionization characteristics in QED environments by Riso *et al.* [59] underlining the critical importance of accurately treating the ionized electron.

Beyond the investigations focused on ionization and electron attachment, numerous studies have utilized QED-CC methodologies to examine the potential impact of vacuum fluctuations within chemical scenarios. It is crucial to emphasize that these studies concern alterations in the ground states of cavity-embedded systems, rather than inducing transitions or generating polariton states by introducing photons into the cavity.

Pavošević *et al.* [53] employed a non-unitary QED-

TABLE III: Comparison of QED-HF ground state energy and the correlation energy calculated at various CCSD(m, n) levels for the Malonaldehyde molecule using cc-pVDZ and aug-cc-pVDZ basis sets. The calculations were performed with three different polarizations, λ_x , λ_y , and λ_z , set to 0.1, and Ω_{cav} set to 3.0 eV.

Method	X-polarization		Y-polarization		Z-polarization	
	cc-pVDZ	aug-cc-pVDZ	cc-pVDZ	aug-cc-pVDZ	cc-pVDZ	aug-cc-pVDZ
QED-HF	-265.559 2463	-265.575 7048	-265.557 9089	-265.574 9429	-265.577 3076	-265.593 1532
QED-CCSD(2, 0)	-0.817 9788	-0.857 4507	-0.820 9197	-0.859 2885	-0.816 3715	-0.857 8009
QED-CCSD(2, 1)	-0.826 4511	-0.866 8022	-0.828 9601	-0.867 9947	-0.820 1303	-0.863 5767
QED-CCSD(2, 2)	-0.827 2880	-0.867 8472	-0.829 6532	-0.868 8461	-0.820 2708	-0.863 9477

TABLE IV: Comparison of QED-HF ground state energy and the correlation energy calculated at various CCSD(m, n) levels for the Aminopropenal molecule using cc-pVDZ and aug-cc-pVDZ basis sets. The calculations were performed with three different polarizations, λ_x , λ_y , and λ_z , set to 0.1, and Ω_{cav} set to 3.0 eV.

Method	X-polarization		Y-polarization		Z-polarization	
	cc-pVDZ	aug-cc-pVDZ	cc-pVDZ	aug-cc-pVDZ	cc-pVDZ	aug-cc-pVDZ
QED-HF	-245.724 0393	-245.740 0942	-245.721 9344	-245.738 4659	-245.743 1042	-245.758 3281
QED-CCSD(2, 0)	-0.808 3272	-0.846 4789	-0.812 2811	-0.849 1371	-0.807 0122	-0.847 1832
QED-CCSD(2, 1)	-0.817 6584	-0.856 7412	-0.821 0162	-0.858 6250	-0.811 0344	-0.853 5370
QED-CCSD(2, 2)	-0.818 6910	-0.858 0266	-0.821 8357	-0.859 6684	-0.811 1960	-0.853 9951

CCSD-2 approach to demonstrate that strong coupling can lead to significant changes in proton transfer reaction barrier heights. The authors also introduced an approximation to QED-CCSD-2, where single electron transitions are paired with up to two photon creation operators, while double electron transitions are associated with single photon creation operators (referred to as QED-CCSD-21). This QED-CCSD-21 model bears resemblance to the method developed by White *et al.* [60], which is designed to simulate electron-phonon interactions.

Pašević and Rubio [29] incorporated QED-CCSD-1 into an embedding protocol. This approach focuses on a portion of a cavity-embedded molecular system using QED-CC, while the remaining part of the system is analyzed using either QED-DFT or QED-HF, termed as "QED-CC-in-QED-SCF". Assuming that electron-photon correlations are localized within the embedded region, this novel protocol could potentially alleviate the computational complexities inherent in the many-body *ab initio* cavity QED framework. We refer to an excellent review article by DePrince *et al.* [61] for a more elaborate discussion on various *Ab initio* methods for polariton chemistry.

In this article, we present our implementation of the QED-CC method using the Pauli-Fierz Hamiltonian. Our approach employs a coherent state basis and incorporates both single and double excitations, covering both individual and mixed excitations. This implementation is carried out on the ExaChem platform [62], a parallel heterogeneous computing platform. ExaChem is built upon the Tensor Algebra for Many-body Methods (TAMM) [63], a specialized tensor library designed

explicitly for the development of quantum chemistry applications and tailored for modern computing platforms, applicable to both CPUs and various GPUs.

The introduction provides an overview of the rationale behind integrating QED effects into the CCSD framework. It also highlights the significant advancements made in enhancing the accuracy of quantum simulations in prior research. The remainder of this paper is as follows: In Sec. II, we briefly describe the QED-CC method within the single and double excitation approximation for both electronic and bosonic degrees of freedom. Sec. III provides a brief overview of the details of the implementation within the ExaChem [62] program package. Sec. IV and Sec. V are reserved for details of computational variables and parameters, and subsequent result and discussion section that includes parallel performance, before making final comments in Sec. VI. We consistently use atomic units throughout this article unless otherwise specified.

II. METHOD

A. Coupled-Cluster theory for Electrons

We consider a system of N electrons described by the electronic Hamiltonian H^e given by:

$$H^e = \sum_{i=1}^N h(r_i, p_i) + \sum_{i=1}^{N-1} \sum_{j=i+1}^N \frac{1}{|r_i - r_j|}, \quad (1)$$

where r_i and p_i represent the position and canonical momentum of electron i , respectively. The second quantized

form of the Hamiltonian is given by:

$$H^e = h_\nu^\mu E_\nu^\mu + \frac{1}{2} u_{\nu\lambda}^{\mu\gamma} E_{\nu\lambda}^{\mu\gamma}, \quad (2)$$

where $E_\nu^\mu = c_\mu^\dagger c_\nu$ and $E_{\nu\lambda}^{\mu\gamma} = c_\mu^\dagger c_\gamma^\dagger c_\lambda c_\nu$ with c_μ^\dagger (c_μ) being a creation (annihilation) operator in a complete, orthonormal set of $2n_{\text{basis}}$ spin-orbitals $\{\psi_\mu\}$, where n_{basis} is the number of basis functions,

$$h_\nu^\mu = \int dx_1 \psi_\mu^*(x_1) h(r_1, p_1) \psi_\nu(x_1), \quad (3)$$

$$u_{\nu\lambda}^{\mu\gamma} = \iint dx_1 dx_2 \frac{\psi_\mu^*(x_1) \psi_\gamma^*(x_2) \psi_\nu(x_1) \psi_\lambda(x_2)}{|r_1 - r_2|}, \quad (4)$$

where $x_i = (r_i, \sigma_i)$ is a composite spatial-spin coordinate.

The ground-state wave function in the CC method [43–47] is defined as

$$|\Psi\rangle = e^T |0^e\rangle, \quad (5)$$

where $|0^e\rangle$ denotes a single Slater determinant, which is typically, but not always, the N -electron Hartree-Fock reference determinant. T represents the cluster operator. When applied to the reference determinant, it generates excited determinants that encompass correlated determinantal configurations, thereby accounting for electron correlations.

The fermionic cluster operators are expressed as follows:

$$\begin{aligned} T &= T_1 + T_2 + \dots, \\ &= \sum_{i,a} t_i^a E_i^a + \sum_{a<b, i<j} t_{ij}^{ab} E_{ij}^{ab} + \dots \end{aligned} \quad (6)$$

Here, the excitation operators T_1 , T_2 , and so on, generate singly and doubly excited determinants, and so forth, when acting on the reference function $|0^e\rangle$.

The indices i, j and a, b refer to the occupied and virtual spin-orbitals, respectively, with respect to the reference determinant. Hereafter, we will simply refer to them as orbitals.

Premultiplying the electronic Schrödinger equation involving the CC wavefunction $H^e e^T |0^e\rangle = E e^T |0^e\rangle$ by the nonsingular operator e^{-T} and projecting it onto the basis of excited determinants $|\Phi_{ij\dots}^{ab\dots}\rangle$ relative to the N -electron Hartree-Fock determinant, we obtain the equations for the amplitudes:

$$\langle \Phi_{ij\dots}^{ab\dots} | e^{-T} H^e e^T |0^e\rangle = 0. \quad (7)$$

These are coupled, nonlinear, simultaneous equations that are solved iteratively. Finally, the ground-state energy can be obtained from the energy expression of Eq. 8 using the solved amplitudes obtained within a certain given threshold.

$$E_{CC} = \langle 0^e | e^{-T} H^e e^T |0^e\rangle. \quad (8)$$

B. Unified Coupled-Cluster Framework for Electron-Photon Interactions

In general, the interactions between molecules and photons within an optical cavity are typically modeled using the Pauli-Fierz Hamiltonian [7, 64–66]. To incorporate the optical cavity, we couple the electronic system to a single photon mode. We utilize the dipole approximation, which is justified by the significant disparity between the wavelength of the photon mode and the dimensions of our molecular system. Additionally, we adopt the coherent state basis to facilitate our implementation. Given these assumptions, and following the prescription of Haugland *et al.* [55], the Pauli-Fierz Hamiltonian takes the following form:

$$\begin{aligned} H &= H_e + \Omega_{\text{cav}} b^\dagger b - \sqrt{\frac{\Omega_{\text{cav}}}{2}} (\lambda \cdot (\mathbf{d} - \langle \mathbf{d} \rangle)) (b^\dagger + b) \\ &\quad + \frac{1}{2} (\lambda \cdot (\mathbf{d} - \langle \mathbf{d} \rangle))^2 \end{aligned} \quad (9)$$

Here, H_e is the standard molecular electronic Hamiltonian within the Born-Oppenheimer approximation defined in Eq. 2. The second term in the Hamiltonian represents the photonic part, modeled by a harmonic oscillator with Ω_{cav} as the fundamental frequency, and b^\dagger and b are bosonic creation and annihilation operators, respectively.

The third term is the bi-linear coupling that couples fermionic and bosonic degrees of freedom with a coupling strength vector λ . The value of λ is related to the field strength of the photon mode. The coupling strength λ can be defined by an effective volume V_{eff} . Specifically, λ is given by $\lambda = \sqrt{\frac{1}{\epsilon_0 V_{\text{eff}}}}$ [15, 67], where ϵ_0 is the vacuum permittivity.

The last term in the Hamiltonian is the dipole self-energy, which ensures that the Hamiltonian is bounded from the below and is origin-independent [66, 68–70]. \mathbf{d} is the molecular dipole operator given by $\mathbf{d} = d_q^p E_q^p$ with $d_q^p = \langle p | \mathbf{d}_e + \frac{\mathbf{d}_{\text{nuc}}}{N_e} | q \rangle$, where \mathbf{d}_e is electronic dipole moment and

$$\mathbf{d}_{\text{nuc}} = \sum_A Z_A \mathbf{R}_A \quad (10)$$

is the nuclear component. Here, Z_A is the nuclear charge, \mathbf{R}_A is the nuclear displacement vector of atomic nucleus A , and N_e is the total number of electrons under consideration. The nuclear dipole moment does not contribute to the Hamiltonian in the coherent-state basis. However, it appears in the wavefunction through the coherent-state transformation. For details, see Ref. [55].

This Hamiltonian is origin invariant for neutral systems; however, it is not origin invariant for charged systems, where the origin dependence arises from the dipole operator [55]. The error or change in the ground state energy due to the origin dependence can be minimized by placing the molecule at the center of its mass.

The starting point for the QED-CC method is a QED-HF reference wavefunction, which extends the electronic

HF method. The QED reference wavefunction is defined as [55, 71],

$$|R\rangle = |0^e\rangle \otimes |0^{ph}\rangle \quad (11)$$

This is a direct product of the electronic ($|0^e\rangle$) and photonic ($|0^{ph}\rangle$) reference wavefunctions.

The wavefunction in the QED-CC method is defined as [55],

$$|\Psi_{\text{QED-CC}}\rangle = e^{T(e,ph)}|R\rangle \quad (12)$$

The notation e and ph within the parentheses of the T operator correspond to electronic and photonic excitation manifolds from the reference wavefunction. The cluster operator $T = \sum_{\mu,n} t_{\mu,n} a^\mu (b^\dagger)^n$ consists of unknown parameters that are determined by solving a set of nonlinear equations [55, 72],

$$\langle R|a_\mu(b)^n e^{-T} H e^T |R\rangle = \sigma_{\mu,n} = 0 \quad (13)$$

Here, $a^\mu = a_\mu^\dagger = \{E_i^a, E_{ij}^{ab}, \dots\}$ represents the electronic excitation operator. The index μ indicates the electronic excitation rank, and n denotes the number of photons.

III. IMPLEMENTATION WITHIN EXACHEM

The way the dipole self-energy term is applied varies across different studies due to different treatments of the squared electric dipole operator. To understand these discrepancies, let's begin by expanding the dipole self-energy operator as follows:

$$\begin{aligned} \frac{1}{2}[\lambda \cdot (\mathbf{d} - \langle \mathbf{d} \rangle)]^2 &= \frac{1}{2}(\lambda \cdot \mathbf{d})^2 - (\lambda \cdot \mathbf{d})(\lambda \cdot \langle \mathbf{d} \rangle) \\ &\quad + \frac{1}{2}(\lambda \cdot \langle \mathbf{d} \rangle)^2 \end{aligned} \quad (14)$$

The square of the electric dipole operator, which is the first term on the right-hand side of Eq. 14, can be expanded into contributions from one-electron and two-electron terms as follows:

$$\begin{aligned} (\lambda \cdot \mathbf{d})^2 &= \sum_{i \neq j} [\lambda \cdot \mathbf{d}(i)][\lambda \cdot \mathbf{d}(j)] + \sum_i [\lambda \cdot \mathbf{d}(i)]^2 \quad (15) \\ &= \lambda^2 \sum_{\mu\nu\lambda\sigma} \mathbf{d}_\nu^\mu \mathbf{d}_\sigma^\lambda E_{\sigma\nu}^{\mu\lambda} - \lambda^2 \sum_{\mu\nu} Q_\nu^\mu E_\nu^\mu \quad (16) \end{aligned}$$

The symbols \mathbf{d}_ν^μ and Q_ν^μ represent electric dipole and electric quadrupole integrals, which have the form:

$$\langle \mu | d_e | \nu \rangle = - \int \phi_\mu^*(\mathbf{r}_1) \mathbf{r}_1 \phi_\nu(\mathbf{r}_1) d\mathbf{r}_1 \quad (17)$$

$$\langle \mu | Q | \nu \rangle = - \int \phi_\mu^*(\mathbf{r}_1) \mathbf{r}_1 \mathbf{r}_2 \phi_\nu(\mathbf{r}_2) d\mathbf{r}_1 d\mathbf{r}_2 \quad (18)$$

On the other hand, numerous studies interpret the second-quantized form of the square of the electric dipole operator as the product of second-quantized electric dipole operators [55], which leads to

$$(\lambda \cdot \mathbf{d})^2 = \lambda^2 \sum_{\mu\nu\lambda\sigma} \mathbf{d}_\nu^\mu \mathbf{d}_\sigma^\lambda E_{\sigma\nu}^{\mu\lambda} + \lambda^2 \sum_{\mu\nu} \sum_{\sigma} \mathbf{d}_\sigma^\mu \mathbf{d}_\nu^\sigma E_\lambda^{\mu\nu} \quad (19)$$

Taking into account of the expansion of the square of the dipole operator, we rewrite the Pauli-Fierz Hamiltonian as,

$$\begin{aligned} H &= H'_e + \Omega_{\text{cav}} b^\dagger b - \sqrt{\frac{\Omega_{\text{cav}}}{2}} (\lambda \cdot (\mathbf{d} - \langle \mathbf{d} \rangle)) (b^\dagger + b) \\ &\quad + \frac{1}{2} (\lambda \cdot \langle \mathbf{d} \rangle)^2 \end{aligned} \quad (20)$$

Here, H'_e is

$$\begin{aligned} H'_e &= (h_q^p - \frac{1}{2} \lambda^2 \cdot Q_q^p - \langle \mathbf{d} \rangle \cdot \mathbf{d}) E_q^p \\ &\quad + \frac{1}{2} \lambda^2 \cdot (u_{qs}^{pr} + \mathbf{d}_q^p \otimes \mathbf{d}_s^r) E_{qs}^{pr} \end{aligned} \quad (21)$$

When averaging over the photon vacuum state $|0^{ph}\rangle$, the PF Hamiltonian of Eq. 20 takes the form for the QED-HF procedure as follows [55]:

$$\langle H \rangle_{0^{ph}} = H'_e + \frac{1}{2} (\lambda \cdot \langle \mathbf{d} \rangle)^2 \quad (22)$$

This procedure allows one to avoid optimizing photonic orbitals at the QED-HF level. With minor modifications to the existing electronic HF code, one can solve for the QED-HF reference wavefunction. The purely photonic part of the Hamiltonian and the bi-linear coupling term should be taken into account at the post-Hartree-Fock level.

The truncation of the cluster operator at a certain excitation rank m and number of photons n establishes the QED-CC hierarchy. Throughout this paper, we adopt the QED-CCSD(m, n) notation, which represents the highest degree of interactions involving m electrons with n photons. Below, these notations are presented in equation form:

$$\begin{aligned}
& \overbrace{\overbrace{\overbrace{}^{\text{CCSD(2,0)}}}^{\text{CCSD(2,1)}}}^{\text{CCSD(2,2)}} \\
T(e, ph) &= T(1,0) + T(2,0) + T(0,1) + T(1,1) + T(2,1) + T(0,2) + T(1,2) + T(2,2) \quad (23) \\
&= t_i^{a,0} E_i^a + t_{ij}^{ab,0} E_{ij}^{ab} + t^{0,1} b^\dagger + t_i^{a,1} E_i^a b^\dagger + t_{ij}^{ab,1} E_{ij}^{ab} b^\dagger + t^{0,2} b^\dagger b^\dagger + t_i^{a,2} E_i^a b^\dagger b^\dagger + t_{ij}^{ab,2} E_{ij}^{ab} b^\dagger b^\dagger \quad (24)
\end{aligned}$$

We have devised three approximate schemes to understand how photon-electron interactions influence the electronic ground state. We denote these approximate schemes as CCSD(2, 0), CCSD(2, 1), and CCSD(2, 2). The CCSD(2, 0) involves performing electronic CCSD calculations with the QED Fock matrix elements and two-electron integrals that are transformed using the coefficient matrix elements obtained from the QED-HF procedure.

We can also obtain the same results as CCSD(2, 0) by setting $\Omega_{\text{cav}} = 0$ in either CCSD(2, 1) or CCSD(2, 2). The parameter Ω_{cav} is inversely proportional to the length of the cavity, L ($\Omega_{\text{cav}} \propto \frac{1}{L}$), meaning it is essentially performing QED-CCSD(m, n) simulations with a cavity of infinite length.

CCSD(2, 0) does not require any new amplitude tensor definitions; the electronic T_1 and T_2 are sufficient. However, the CCSD(2, 1) scheme requires a total of five kinds of amplitude tensors, namely $T(1,0)$, $T(2,0)$, $T(0,1)$, $T(1,1)$, and $T(2,1)$. The CCSD(2, 2) requires an additional three new tensors $T(0,2)$, $T(1,2)$, and $T(2,2)$. Out of these, $T(0,1)$ and $T(0,2)$ are rank-zero tensors or scalars. Since the bosonic part is a scalar, the mixed tensors $T(1,1)$, $T(2,1)$, $T(1,2)$, and $T(2,2)$ do not increase any dimensionality in the tensor definition. Therefore, the computational complexity for all the schemes remains the same as the electronic CCSD method of N^6 ; however, these schemes increase the prefactors in the computational complexity. As pointed out earlier, the nuclear dipole moment does not contribute to the Hamiltonian in the coherent-state basis. However, we observed that the inclusion of the $\frac{d_{\text{nuc}}}{N_e}$ term in the Hamiltonian results in more stable convergence at both the SCF and CC levels.

We have implemented the QED-CC method within the ExaChem program package [62], which is a freely distributed open-source software. ExaChem is built upon the Tensor Algebra for Many-body Methods (TAMM) infrastructure [63]. TAMM is a massively parallel, heterogeneous tensor algebra library designed for scalable performance. It supports portable implementations of many-body methods on current and future exascale supercomputing platforms. TAMM enables users to specify and manage tensor distribution, memory, and operation scheduling, and supports both complex and mixed real-complex algebra. It utilizes Global Arrays [73] and MPI for scalable parallelization on distributed memory systems, along with optimized libraries for efficient intranode execution on CPUs and accelerators. For GPU ex-

ecution, TAMM uses localized summation loops to minimize data transfer between GPUs and CPUs, thereby reduce CPU-GPU data transmission.

IV. COMPUTATIONAL DETAILS

In this article, we report results for several closed-shell molecules, namely hydrogen, water, malonaldehyde, and aminopropenal, using various basis sets. For hydrogen and water molecules, we have used experimental geometries. The geometries of malonaldehyde and aminopropenal are taken from Ref. [53] and were optimized at the electronic CCSD level using the cc-pVDZ [74] basis set.

The hydrogen molecule serves as a reference system for comparing the accuracy of our CCSD(2, 2) implementation with the QED-FCI method, as detailed in [42]. We utilized cc-pVDZ [74], aug-cc-pVDZ [75], cc-pVTZ [74], and aug-cc-pVTZ [75] basis sets for both hydrogen in the hydrogen molecule and hydrogen and oxygen in water. To validate our implementation further, we compared our results for water molecules with those obtained using the code by Flick et al. [53].

For hydrogen, carbon, and oxygen in the malonaldehyde molecule, we employed the cc-pVDZ [74] and aug-cc-pVDZ [75] basis sets. Similarly, for the aminopropenal molecule, we used the cc-pVDZ [74] and aug-cc-pVDZ [75] basis sets for hydrogen, carbon, nitrogen, and oxygen atoms. We also report results for variations in ground-state energy by varying either λ or Ω_{cav} while keeping the other constant, using aminopropenal as an example.

The necessary matrix elements for implementing the QED-CCSD(m, n) methods within the ExaChem [62] infrastructure are taken from the libint2.9.0 integral engine. We used an integral threshold of 10^{-20} and a linear dependence threshold of 10^{-5} in all our simulations. At the SCF level, we employed a threshold of 10^{-9} for density and 10^{-8} Frobenius norm of the residual vector unless specifically reported. All calculations used a direct inversion in the iterative subspace (DIIS) of 5. None of the electrons were frozen in any of our calculations.

V. RESULTS AND DISCUSSION

To verify the correctness of our implementation, we conducted various tests. One such test compared the

results from our ExaChem implementation of the QED-CCSD(2, 2) method with the developmental version of the QED-CCSD-mn methods by Flick [53], available as supplemental material in Ref. [53]. We used water molecule with experimental geometry as the test case across various basis sets, with $\lambda_z = 0.1$ and $\Omega_{\text{cav}} = 3.0$ eV, ranging from cc-pVDZ to aug-cc-pVTZ. The choice of cavity parameters is arbitrary. The results are summarized in Table I. The QED-CCSD-mn simulations were performed using a MacBook Pro with 16 GB of RAM having Apple M1 chip, which is insufficient to simulate even a water molecule using the aug-cc-pVTZ basis set, and therefore, it is not reported in the table. We conducted many other tests by varying Ω_{cav} or the direction of the polarization with various coupling strengths. In all cases, we achieved nine to ten digits of agreement after the decimal for the SCF method and seven to eight digits of agreement for the CCSD(2, 2), irrespective of the simulation conditions. The discrepancy beyond this limit is due to the fact that the two codes use different convergence algorithms. The code of Ref. [53] uses a convergence threshold over difference in correlation energy between two successive iterations, whereas we use a threshold over the maximum of the Frobenius norm of the residual vectors.

Furthermore, we have compared our QED-CCSD(2, 2) results for a two-electron system with values computed using the coherent-state quantum electrodynamics version of full configuration interaction (CS-QED-FCI)[42]. Theoretically, the coherent-state basis represents an infinite photon occupation. However, CS-QED-FCI has the option to use finite photon occupation. The CS-QED-FCI results are reported with converged photon occupation. We used hydrogen molecule at its experimental bond length of 0.74 Å. The molecule is oriented in the z -direction with one of the hydrogens placed at the (0, 0, 0) coordinate so that there is a non-zero dipole moment in the direction of polarization. We have used coupling strength $\lambda_z = 0.05$ and $\Omega_{\text{cav}} = 20.0$ eV in all our comparisons. Here also, we employed cc-pVDZ to aug-cc-pVTZ basis sets for computing ground state energy using the QED-CCSD(2, 2) method. We obtained perfect agreement with QED-FCI [42] values wherever it was possible to compute. The results are reported in Tab II

In Fig. 1, we report the results of shifting the Z -coordinate and the ground-state energy computed at the QED-HF and QED-CCSD(2, 2) levels. The hydrogen molecule is oriented in the z -direction, with one of the hydrogen atoms placed at the center of the coordinate system to ensure a non-zero dipole moment in that direction. We employed $\lambda_z = 0.05$ and $\Omega_{\text{cav}} = 20.0$ eV using the aug-cc-pVDZ basis set. We gradually shifted the Z -coordinate starting with 1 Å to 16 Å. We observed no change in the QED-HF or QED-CCSD(2, 2) correlation energies. Therefore, we can conclude that our implementation is origin-invariant.

In Table III, we present results for the malonaldehyde molecule using cc-pVDZ and aug-cc-pVDZ basis

sets with QED-CCSD(m, n) schemes, considering either X-, Y-, or Z-polarization with a coupling strength of 0.1. In all cases, we used $\Omega_{\text{cav}} = 3.0$ eV. The electronic SCF energy of the molecule is -265.6559200 in the cc-pVDZ basis set and -265.6734631 in the aug-cc-pVDZ basis set. The purely electronic correlation energy changes from -0.8024509 to -0.8399609 when switching from the cc-pVDZ basis set to the aug-cc-pVDZ basis set.

The QED-HF ground state energy for X-polarization is -265.5592463 with the cc-pVDZ basis set and -265.5757048 with the aug-cc-pVDZ basis set. For Y-polarization, the QED-HF ground state energy is -265.5579089 with the cc-pVDZ basis set and -265.5749429 with the aug-cc-pVDZ basis set. For Z-polarization, the QED-HF ground state energy is -265.5773076 with the cc-pVDZ basis set and -265.5931532 with the aug-cc-pVDZ basis set.

The QED-CCSD correlation energies for the (2,0) level are -0.8179788 (cc-pVDZ) and -0.8574507 (aug-cc-pVDZ) for X-polarization, -0.8209197 (cc-pVDZ) and -0.8592885 (aug-cc-pVDZ) for Y-polarization, and -0.8163715 (cc-pVDZ) and -0.8578009 (aug-cc-pVDZ) for Z-polarization. For the (2,1) level, the QED-CCSD correlation energies are -0.8264511 (cc-pVDZ) and -0.8668022 (aug-cc-pVDZ) for X-polarization, -0.8289601 (cc-pVDZ) and -0.8679947 (aug-cc-pVDZ) for Y-polarization, and -0.8201303 (cc-pVDZ) and -0.8635767 (aug-cc-pVDZ) for Z-polarization. For the (2,2) level, the QED-CCSD correlation energies are -0.8272880 (cc-pVDZ) and -0.8678472 (aug-cc-pVDZ) for X-polarization, -0.8296532 (cc-pVDZ) and -0.8688461 (aug-cc-pVDZ) for Y-polarization, and -0.8202708 (cc-pVDZ) and -0.8639477 (aug-cc-pVDZ) for Z-polarization.

The ground state energy obtained from QED-HF calculations is lower (more negative) when using the aug-cc-pVDZ basis set compared to the cc-pVDZ basis set across all polarizations. This suggests that the aug-cc-pVDZ basis set, being larger and more complete, provides a more accurate representation of the electronic structure. The correlation energy, which accounts for electron correlation effects beyond the mean-field approximation, also shows more negative values with the aug-cc-pVDZ basis set compared to the cc-pVDZ basis set. This trend is consistent across different levels of QED-CCSD (2,0), (2,1), and (2,2) and different polarizations. The correlation energy values indicate that the electron correlation is better captured with the more comprehensive aug-cc-pVDZ basis set. The results show slight variations in energies depending on the polarization direction (X, Y, or Z). For instance, the Z-polarization often results in slightly more negative QED-HF energies compared to X and Y polarizations, which could be indicative of specific interactions between the electronic structure of malonaldehyde and the electromagnetic field in that direction. Overall, the table highlights the importance of basis set selection and polarization in obtaining accurate quantum chemical calculations, with the aug-cc-pVDZ basis

set generally providing better results.

In Table IV, we present the results for the aminopropenal molecule using cc-pVDZ and aug-cc-pVDZ basis sets with QED-CCSD(m, n) schemes, considering X-, Y-, or Z-polarization with a coupling strength of 0.1. In all cases, $\Omega_{\text{cav}} = 3.0$ eV. This molecule has a convergence difficulty when the polarization is applied along the Y-direction. All Y-polarization results are calculated using a threshold of 10^{-6} .

The QED-HF ground state energy for X-polarization is -245.7240393 with the cc-pVDZ basis set and -245.7400942 with the aug-cc-pVDZ basis set. For Y-polarization, the QED-HF ground state energy is -245.7219344 with the cc-pVDZ basis set and -245.7384659 with the aug-cc-pVDZ basis set. For Z-polarization, the QED-HF ground state energy is -245.7431042 with the cc-pVDZ basis set and -245.7583281 with the aug-cc-pVDZ basis set. The electronic SCF energy of the aminopropenal molecule is -245.8268167 with the cc-pVDZ basis set and -245.8443871 with the aug-cc-pVDZ basis set. The purely electronic correlation energy changes from -0.7917050 to -0.82750579 when switching from the cc-pVDZ basis set to the aug-cc-pVDZ basis set.

The QED-CCSD correlation energies for the (2,0) level are -0.8083272 (cc-pVDZ) and -0.8464789 (aug-cc-pVDZ) for X-polarization, -0.8122811 (cc-pVDZ) and -0.8491371 (aug-cc-pVDZ) for Y-polarization, and -0.8070122 (cc-pVDZ) and -0.8471832 (aug-cc-pVDZ) for Z-polarization. For the (2,1) level, the QED-CCSD correlation energies are -0.8176584 (cc-pVDZ) and -0.8567412 (aug-cc-pVDZ) for X-polarization, -0.8210162 (cc-pVDZ) and -0.8586250 (aug-cc-pVDZ) for Y-polarization, and -0.8110344 (cc-pVDZ) and -0.8535370 (aug-cc-pVDZ) for Z-polarization. For the (2,2) level, the QED-CCSD correlation energies are -0.8186910 (cc-pVDZ) and -0.8580266 (aug-cc-pVDZ) for X-polarization, -0.8218357 (cc-pVDZ) and -0.8596684 (aug-cc-pVDZ) for Y-polarization, and -0.8111960 (cc-pVDZ) and -0.8539951 (aug-cc-pVDZ) for Z-polarization.

The QED-HF calculations consistently yield lower (more negative) ground state energies when employing the aug-cc-pVDZ basis set compared to the cc-pVDZ basis set across all polarizations. This suggests that the aug-cc-pVDZ basis set, being more extensive and comprehensive, provides a more accurate representation of the electronic structure. Furthermore, the correlation energy, which accounts for electron correlation effects beyond the mean-field approximation, also demonstrates more negative values with the aug-cc-pVDZ basis set compared to the cc-pVDZ basis set. This trend persists across various levels of QED-CCSD (2,0), (2,1), and (2,2), as well as different polarizations. The correlation energy values indicate that the electron correlation is better captured with the more sophisticated aug-cc-pVDZ basis set.

The results exhibit slight energy variations depending

on the polarization direction (X, Y, or Z). For instance, Z-polarization often yields slightly more negative QED-HF energies compared to X and Y polarizations, implying potential specific interactions between the electronic structure of aminopropenal and the electromagnetic field in that direction. Overall, the table underscores the importance of both basis set selection and polarization in achieving accurate quantum chemical calculations, with the aug-cc-pVDZ basis set generally providing superior results.

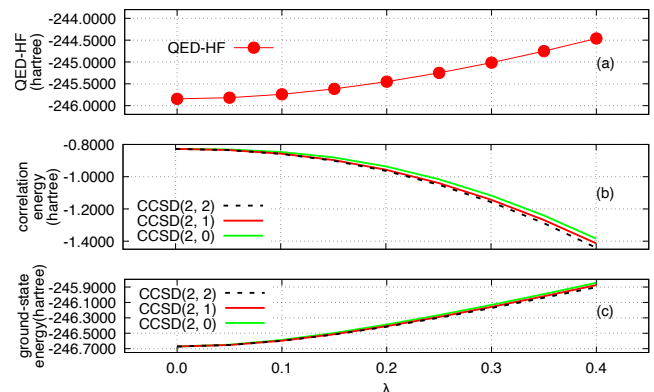


FIG. 2: Variation of QED-HF ground state energy (a), correlation energies using various CCSD(m, n) schemes (b), and total ground-state energy at the QED-CCSD(m, n) levels (c) with the variation in λ_x , while keeping $\Omega_{\text{cav}} = 3.0$ eV using the aug-cc-pVDZ basis set.

The results depicted in Fig. 2 show the variation of QED-HF ground state energy, correlation energies using different CCSD(m, n) schemes, and total ground state energy at the QED-CC levels with respect to the polarization parameter λ_x . These calculations were conducted using the aug-cc-pVDZ [75] basis set with a fixed cavity frequency of $\Omega_{\text{cav}} = 3.0$ eV.

As λ_x increases from 0 to 0.4, there is a consistent decrease in the QED-HF ground state energy. This indicates a stronger interaction between the molecular system and the electromagnetic field along the x-direction. When $\lambda_x = 0$, the system's behavior essentially reflects the effects outside of the cavity, or in other words, these effects are of purely electronic origin.

In contrast to the QED-HF energy, the correlation energy computed using various CCSD(m, n) schemes shows an opposite trend. There is an increase in the correlation energy with the increase in the electron-photon coupling strength. Among the three approximation schemes, the CCSD(2, 2) scheme exhibits the largest increase in correlation energy, while the CCSD(2, 1) scheme shows a moderate increase. This suggests that higher-order electron correlation effects become more pronounced with stronger coupling to the photon field. Despite the opposing trends in QED-HF and QED-CCSD(m, n) correlation energies, the overall ground state energy at the QED-

CCSD(m, n) level decreases with increasing λ_x . This implies that the total electronic ground state is significantly influenced by the degree of polarization. The observed decrease in ground state energy, despite the opposing trends in individual energy components, highlights the complex interplay between electronic and photonic interactions in the system. It underscores the necessity of using advanced quantum electrodynamic methods to accurately model these interactions. The results demonstrate the sensitivity of the molecular system’s properties to external electromagnetic fields and polarization parameters, emphasizing the importance of precise modeling for reliable predictions of molecular properties. In summary, the data reveal that while the QED-HF ground state energy decreases with increasing λ_x , the correlation energies increase, particularly for higher-order CCSD schemes. This results in an overall decrease in the total ground state energy at the QED-CCSD level, illustrating the nuanced effects of electron-photon coupling on the electronic structure. Such insights are crucial for developing accurate quantum chemical methods that account for the influence of external fields and polarization effects.

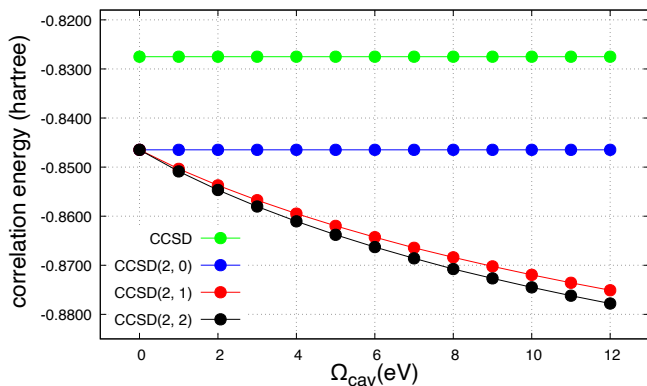


FIG. 3: Variation of correlation energies using various CCSD(m, n) schemes as a function of Ω_{cav} , while keeping $\lambda_x = 0.1$, using the aug-cc-pVDZ basis set.

The results depicted in Fig. 3 using aug-cc-pvDZ [75] basis set illustrate the correlation energies for the CCSD(2, 1) and CCSD(2, 2) methods across various values of the parameter Ω_{cav} . The correlation energy for the standard CCSD method remains constant at -0.8275058 , while the CCSD(2, 0) correlation energy remains steady at -0.8464789 , as they are independent of the Ω_{cav} value. The SCF energy for purely electronic degrees of freedom is -245.844381 , and for the QED-HF case, it is -245.7400942 . The QED-SCF energy also does not vary with the employed Ω_{cav} .

The correlation energy for the CCSD(2, 1) method decreases with increasing Ω_{cav} , starting from -0.8464789 at $\Omega_{cav} = 0$ and decreasing to -0.8750895 at $\Omega_{cav} = 12$. This indicates that the CCSD(2, 1) method is responsive to changes in Ω_{cav} , capturing more electron-photon

interaction as Ω_{cav} increases. Similarly, the correlation energy for the CCSD(2, 2) method decreases with increasing Ω_{cav} , starting from -0.8464789 at $\Omega_{cav} = 0$ and decreasing to -0.8777892 at $\Omega_{cav} = 12$. The CCSD(2, 2) method exhibits the most significant variation among the methods, suggesting that it comprehensively captures the electron-photon interaction effects.

Both the CCSD(2, 1) and CCSD(2, 2) methods display a decreasing trend in correlation energy with increasing Ω_{cav} , indicating their ability to better capture the dynamics introduced by varying the electron-photon coupling strength. The larger decrease in correlation energy for the CCSD(2, 2) method compared to CCSD(2, 1) suggests that higher-level approximations within the CCSD framework are more effective in capturing the effects of increasing electron-photon interactions.

These findings imply that as the parameter Ω_{cav} increases, the system’s correlation energy decreases, possibly due to enhanced electron-photon interactions. This emphasizes the importance of employing appropriate quantum electrodynamic coupled-cluster methods to accurately model such systems. For precise modeling of systems where electron-photon interactions are significant, higher-level QED-CCSD methods (such as CCSD(2, 1) and CCSD(2, 2)) should be preferred over standard electronic CCSD and CCSD(2, 0) methods. The data provided demonstrates that higher-level QED-CCSD methods, particularly CCSD(2, 1) and CCSD(2, 2), are sensitive to changes in the electron-photon coupling parameter Ω_{cav} , capturing more nuanced interactions and providing more accurate correlation energies, and thereby changes the electronic ground state.

VI. CONCLUSION

In summary, our implementation of the quantum electrodynamics coupled-cluster method with single and double excitations (QED-CCSD) within the ExaChem program package marks a significant advancement in computational quantum chemistry. By leveraging the Tensor Algebra for Many-body Methods (TAMM) infrastructure, our framework offers a scalable and efficient solution for modeling both electronic and bosonic amplitudes, encompassing individual and mixed excitation processes.

This innovative computational framework extends beyond the traditional CCSD method, incorporating the intricate interplay between electronic and bosonic degrees of freedom. Through rigorous theoretical foundations, detailed algorithmic descriptions, and comprehensive numerical benchmarks, we have showcased the capability of our approach in accurately describing quantum phenomena, particularly in systems where electron-photon interactions play a significant role.

Our modeling of electron-photon interactions within an optical cavity, using the Pauli-Fierz Hamiltonian within the dipole approximation, adds a new dimension to quantum chemistry simulations. By integrating QED effects

into the CCSD framework, we have created a more versatile and accurate model for simulating complex quantum systems. This advancement not only enhances our understanding of fundamental physical processes but also opens new avenues for predicting and manipulating various phenomena with unprecedented precision.

ACKNOWLEDGMENTS

The authors acknowledge support from the Center for Many-Body Methods, Spectroscopies, and Dynam-

ics for Molecular Polaritonic Systems (MAPOL) under FWP79715. This support is part of the Computational Chemical Sciences (CCS) program funded by the U.S. Department of Energy, Office of Science, Office of Basic Energy Sciences, Division of Chemical Sciences, Geosciences, and Biosciences at Pacific Northwest National Laboratory (PNNL). PNNL is a multi-program national laboratory operated by Battelle Memorial Institute for the United States Department of Energy under DOE contract number DE-AC05-76RL01830.

-
- [1] T. Helgaker, P. Jorgensen, and J. Olsen, *Molecular electronic-structure theory* (John Wiley & Sons, 2013).
- [2] H.-D. Meyer, F. Gatti, and G. A. Worth, *Multidimensional quantum dynamics: MCTDH theory and applications* (John Wiley & Sons, 2009).
- [3] I. P. Grant, *Relativistic quantum theory of atoms and molecules* (Springer, 2007).
- [4] K. G. Dyall and K. Fægri Jr, *Introduction to relativistic quantum chemistry* (Oxford University Press, 2007).
- [5] C. Chang, V. L. Deringer, K. S. Katti, V. Van Speybroeck, and C. M. Wolverson, Simulations in the era of exascale computing, *Nature Reviews Materials* **8**, 309 (2023).
- [6] K. Kowalski, R. Bair, N. P. Bauman, J. S. Boschen, E. J. Bylaska, J. Daily, W. A. de Jong, T. Dunning Jr, N. Govind, R. J. Harrison, et al., From nwchem to nwchemx: Evolving with the computational chemistry landscape, *Chemical reviews* **121**, 4962 (2021).
- [7] M. Ruggenthaler, N. Tancogne-Dejean, J. Flick, H. Appel, and A. Rubio, From a quantum-electrodynamical light-matter description to novel spectroscopies, *Nature Reviews Chemistry* **2**, 1 (2018).
- [8] H. Hübener, M. A. Sentef, U. De Giovannini, A. F. Kemper, and A. Rubio, Creating stable floquet-weyl semimetals by laser-driving of 3d dirac materials, *Nature communications* **8**, 13940 (2017).
- [9] T. Byrnes, N. Y. Kim, and Y. Yamamoto, Exciton-polariton condensates, *Nature Physics* **10**, 803 (2014).
- [10] D. Basov, M. Fogler, and F. García de Abajo, Polaritons in van der waals materials, *Science* **354**, aag1992 (2016).
- [11] S. Latini, E. Ronca, U. De Giovannini, H. Hübener, and A. Rubio, Cavity control of excitons in two-dimensional materials, *Nano letters* **19**, 3473 (2019).
- [12] A. Thomas, J. George, A. Shalabney, M. Dryzhakov, S. J. Varma, J. Moran, T. Chervy, X. Zhong, E. Devaux, C. Genet, J. A. Hutchison, and T. W. Ebbesen, Ground-state chemical reactivity under vibrational coupling to the vacuum electromagnetic field, *Angewandte Chemie International Edition* **55**, 11462 (2016).
- [13] A. Thomas, L. Lethuillier-Karl, K. Nagarajan, R. M. Vergauwe, J. George, T. Chervy, A. Shalabney, E. Devaux, C. Genet, J. Moran, et al., Tilting a ground-state reactivity landscape by vibrational strong coupling, *Science* **363**, 615 (2019).
- [14] D. Sidler, M. Ruggenthaler, C. Schäfer, E. Ronca, and A. Rubio, A perspective on ab initio modeling of polaritonic chemistry: The role of non-equilibrium effects and quantum collectivity, *The Journal of Chemical Physics* **156**, 030901 (2022).
- [15] J. Galego, C. Climent, F. J. Garcia-Vidal, and J. Feist, Cavity-assisted polaritons and their effects in ground-state chemical reactivity, *Phys. Rev. X* **9**, 021057 (2019).
- [16] J. Galego, F. J. Garcia-Vidal, and J. Feist, Cavity-induced modifications of molecular structure in the strong-coupling regime, *Phys. Rev. X* **5**, 041022 (2015).
- [17] H. Walther, B. T. H. Varcoe, B.-G. Englert, and T. Becker, Cavity quantum electrodynamics, *Reports on Progress in Physics* **69**, 1325 (2006).
- [18] R. F. Ribeiro, L. A. Martínez-Martínez, M. Du, J. Campos-Gonzalez-Angulo, and J. Yuen-Zhou, Polariton chemistry: controlling molecular dynamics with optical cavities, *Chemical science* **9**, 6325 (2018).
- [19] J. A. Campos-Gonzalez-Angulo, R. F. Ribeiro, and J. Yuen-Zhou, Resonant catalysis of thermally activated chemical reactions with vibrational polaritons, *Nature communications* **10**, 4685 (2019).
- [20] D. Gallego-Valencia, L. Mewes, J. Feist, and J. L. Sanz-Vicario, Coherent multidimensional spectroscopy in polariton systems, arXiv preprint arXiv:2403.04734 (2024).
- [21] M. Ruggenthaler, D. Sidler, and A. Rubio, Understanding polaritonic chemistry from ab initio quantum electrodynamics, *Chemical Reviews* **123**, 11191 (2023).
- [22] M. Ruggenthaler, F. Mackenroth, and D. Bauer, Time-dependent kohn-sham approach to quantum electrodynamics, *Phys. Rev. A* **84**, 042107 (2011).
- [23] M. Ruggenthaler, J. Flick, C. Pellegrini, H. Appel, I. V. Tokatly, and A. Rubio, Quantum-electrodynamical density-functional theory: Bridging quantum optics and electronic-structure theory, *Phys. Rev. A* **90**, 012508 (2014).
- [24] C. Pellegrini, J. Flick, I. V. Tokatly, H. Appel, and A. Rubio, Optimized effective potential for quantum electrodynamical time-dependent density functional theory, *Phys. Rev. Lett.* **115**, 093001 (2015).
- [25] J. Flick, C. Schäfer, M. Ruggenthaler, H. Appel, and A. Rubio, Ab initio optimized effective potentials for real molecules in optical cavities: Photon contributions to the molecular ground state, *ACS Photonics* **5**, 992 (2018).
- [26] M. J. T. O. A. R. René Jestädt, Michael Ruggenthaler and H. Appel, Light-matter interactions within the

- ehrenfest–maxwell–pauli–kohn–sham framework: fundamentals, implementation, and nano-optical applications, *Advances in Physics* **68**, 225 (2019).
- [27] J. Flick and P. Narang, Ab initio polaritonic potential-energy surfaces for excited-state nanophotonics and polaritonic chemistry, *The Journal of Chemical Physics* **153**, 094116 (2020).
- [28] N. Vu, G. M. McLeod, K. Hanson, and A. E. I. DePrince, Enhanced diastereocontrol via strong light–matter interactions in an optical cavity, *The Journal of Physical Chemistry A* **126**, 9303 (2022).
- [29] F. Pavošević and A. Rubio, Wavefunction embedding for molecular polaritons, *The Journal of Chemical Physics* **157**, 094101 (2022).
- [30] M. D. Liebenthal, N. Vu, and A. E. I. DePrince, Assessing the effects of orbital relaxation and the coherent-state transformation in quantum electrodynamics density functional and coupled-cluster theories, *The Journal of Physical Chemistry A* **127**, 5264 (2023).
- [31] I. V. Tokatly, Time-dependent density functional theory for many-electron systems interacting with cavity photons, *Phys. Rev. Lett.* **110**, 233001 (2013).
- [32] J. Flick, M. Ruggenthaler, H. Appel, and A. Rubio, Atoms and molecules in cavities, from weak to strong coupling in quantum-electrodynamics (qed) chemistry, Proceedings of the National Academy of Sciences **114**, 3026 (2017).
- [33] I. V. Tokatly, Conserving approximations in cavity quantum electrodynamics: Implications for density functional theory of electron-photon systems, *Phys. Rev. B* **98**, 235123 (2018).
- [34] J. Malave, A. Ahrens, D. Pitagora, C. Covington, and K. Varga, Real-space, real-time approach to quantum-electrodynamical time-dependent density functional theory, *The Journal of Chemical Physics* **157**, 194106 (2022).
- [35] J. Yang, Q. Ou, Z. Pei, H. Wang, B. Weng, Z. Shuai, K. Mullen, and Y. Shao, Quantum-electrodynamical time-dependent density functional theory within Gaussian atomic basis, *The Journal of Chemical Physics* **155**, 064107 (2021).
- [36] J. Yang, Z. Pei, E. C. Leon, C. Wickizer, B. Weng, Y. Mao, Q. Ou, and Y. Shao, Cavity quantum-electrodynamical time-dependent density functional theory within Gaussian atomic basis. II. Analytic energy gradient, *The Journal of Chemical Physics* **156**, 124104 (2022).
- [37] J. McTague and I. Foley, Jonathan J., Non-Hermitian cavity quantum electrodynamics–configuration interaction singles approach for polaritonic structure with ab initio molecular Hamiltonians, *The Journal of Chemical Physics* **156**, 154103 (2022).
- [38] M. Bauer and A. Dreuw, Perturbation theoretical approaches to strong light–matter coupling in ground and excited electronic states for the description of molecular polaritons, *The Journal of Chemical Physics* **158**, 124128 (2023).
- [39] Z.-H. Cui, A. Mandal, and D. R. Reichman, Variational lang–firsov approach plus møller–plesset perturbation theory with applications to ab initio polariton chemistry, *Journal of Chemical Theory and Computation* **20**, 1143 (2024).
- [40] J. D. Mallory and A. E. DePrince, Reduced-density-matrix-based ab initio cavity quantum electrodynamics, *Phys. Rev. A* **106**, 053710 (2022).
- [41] B. M. Weight, S. Tretiak, and Y. Zhang, Diffusion quantum monte carlo approach to the polaritonic ground state, *Phys. Rev. A* **109**, 032804 (2024).
- [42] N. Vu, D. Mejia-Rodriguez, N. P. Bauman, A. Panyala, E. Mutlu, N. Govind, and J. J. Foley IV, Cavity quantum electrodynamics complete active space configuration interaction theory, *Journal of Chemical Theory and Computation* (2024).
- [43] F. Coester, Bound states of a many-particle system, *Nucl. Phys.* **7**, 421 (1958).
- [44] F. Coester and H. Kümmel, Short-range correlations in nuclear wave functions, *Nucl. Phys.* **17**, 477 (1960).
- [45] J. Čížek, On the correlation problem in atomic and molecular systems. calculation of wavefunction components in ursell-type expansion using quantum-field theoretical methods, *J. Chem. Phys.* **45**, 4256 (1966).
- [46] J. Paldus, J. Čížek, and I. Shavitt, Correlation problems in atomic and molecular systems. iv. extended coupled-pair many-electron theory and its application to the bh₃ molecule, *Phys. Rev. A* **5**, 50 (1972).
- [47] H. G. Kümmel, A biography of the coupled cluster method, *Int. J. Mod. Phys. B* **17**, 5311 (2003).
- [48] R. J. Bartlett and M. Musiał, Coupled-cluster theory in quantum chemistry, *Rev. Mod. Phys.* **79**, 291 (2007).
- [49] D. Mukherjee and S. Pal, Use of cluster expansion methods in the open-shell correlation problem, *Adv. Quantum Chem.* **20**, 291 (1989).
- [50] A. I. Krylov, Equation-of-motion coupled-cluster methods for open-shell and electronically excited species: the hitchhiker’s guide to fock space, *Annu. Rev. Phys. Chem.* **59**, 433 (2008).
- [51] P. Piecuch, K. Kowalski, I. S. Pimienta, and M. J. Mcguire, Recent advances in electronic structure theory: Method of moments of coupled-cluster equations and renormalized coupled-cluster approaches, *Int. Rev. Phys. Chem.* **21**, 527 (2002).
- [52] T. D. Crawford and H. F. Schaefer, An introduction to coupled cluster theory for computational chemists, *Rev. Comput. Chem.* **14**, 33 (2000).
- [53] F. Pavošević, S. Hammes-Schiffer, A. Rubio, and J. Flick, Cavity-modulated proton transfer reactions, *Journal of the American Chemical Society* **144**, 4995 (2022).
- [54] U. Mordovina, C. Bungey, H. Appel, P. J. Knowles, A. Rubio, and F. R. Manby, Polaritonic coupled-cluster theory, *Phys. Rev. Res.* **2**, 023262 (2020).
- [55] T. S. Haugland, E. Ronca, E. F. Kjørstad, A. Rubio, and H. Koch, Coupled cluster theory for molecular polaritons: Changing ground and excited states, *Phys. Rev. X* **10**, 041043 (2020).
- [56] I. DePrince, A. Eugene, Cavity-modulated ionization potentials and electron affinities from quantum electrodynamics coupled-cluster theory, *The Journal of Chemical Physics* **154**, 094112 (2021).
- [57] F. Pavošević and J. Flick, Polaritonic unitary coupled cluster for quantum computations, *The Journal of Physical Chemistry Letters* **12**, 9100 (2021).
- [58] J. Tilly, H. Chen, S. Cao, D. Picozzi, K. Setia, Y. Li, E. Grant, L. Wossnig, I. Rungger, G. H. Booth, et al., The variational quantum eigensolver: a review of methods and best practices, *Physics Reports* **986**, 1 (2022).
- [59] R. R. Riso, T. S. Haugland, E. Ronca, and H. Koch, On the characteristic features of ionization in QED environments, *The Journal of Chemical Physics* **156**, 234103 (2022).

- [60] A. F. White, Y. Gao, A. J. Minnich, and G. K.-L. Chan, A coupled cluster framework for electrons and phonons, *The Journal of Chemical Physics* **153**, 224112 (2020).
- [61] I. Foley, Jonathan J., J. F. McTague, and I. DePrince, A. Eugene, Ab initio methods for polariton chemistry, *Chemical Physics Reviews* **4**, 041301 (2023).
- [62] A. Panyala, N. Govind, K. Kowalski, N. Bauman, B. Peng, H. Pathak, E. Mutlu, D. Mejia Rodriguez, S. Xantheas, and S. Krishnamoorthy, *Exachem/exachem*, [Computer Software] <https://doi.org/10.11578/dc.20230628.1> (2023).
- [63] E. Mutlu, A. Panyala, N. Gawande, A. Bagusetty, J. Glabe, J. Kim, K. Kowalski, N. P. Bauman, B. Peng, H. Pathak, J. Brabec, and S. Krishnamoorthy, TAMM: Tensor algebra for many-body methods, *The Journal of Chemical Physics* **159**, 024801 (2023).
- [64] C. Cohen-Tannoudji, J. Dupont-Roc, and G. Grynberg, *Photons and atoms-introduction to quantum electrodynamics* (1997).
- [65] H. Spohn, *Dynamics of charged particles and their radiation field* (Cambridge university press, 2004).
- [66] V. Rokaĵ, D. M. Welakuh, M. Ruggenthaler, and A. Rubio, Light-matter interaction in the long-wavelength limit: no ground-state without dipole self-energy, *Journal of Physics B: Atomic, Molecular and Optical Physics* **51**, 034005 (2018).
- [67] C. Climent, J. Galego, F. J. Garcia-Vidal, and J. Feist, Plasmonic nanocavities enable self-induced electrostatic catalysis, *Angewandte Chemie International Edition* **58**, 8698 (2019).
- [68] C. Schäfer, M. Ruggenthaler, V. Rokaĵ, and A. Rubio, Relevance of the quadratic diamagnetic and self-polarization terms in cavity quantum electrodynamics, *ACS Photonics* **7**, 975 (2020).
- [69] D. De Bernardis, T. Jaako, and P. Rabl, Cavity quantum electrodynamics in the nonperturbative regime, *Phys. Rev. A* **97**, 043820 (2018).
- [70] M. A. D. Taylor, A. Mandal, W. Zhou, and P. Huo, Resolution of gauge ambiguities in molecular cavity quantum electrodynamics, *Phys. Rev. Lett.* **125**, 123602 (2020).
- [71] N. Rivera, J. Flick, and P. Narang, Variational theory of nonrelativistic quantum electrodynamics, *Physical review letters* **122**, 193603 (2019).
- [72] R. J. Bartlett and M. Musiał, Coupled-cluster theory in quantum chemistry, *Reviews of Modern Physics* **79**, 291 (2007).
- [73] J. Nieplocha, B. Palmer, V. Tipparaju, M. Krishnan, H. Trease, and E. Aprà, Advances, applications and performance of the global arrays shared memory programming toolkit, *The International Journal of High Performance Computing Applications* **20**, 203 (2006).
- [74] T. H. Dunning Jr, Gaussian basis sets for use in correlated molecular calculations. i. the atoms boron through neon and hydrogen, *The Journal of chemical physics* **90**, 1007 (1989).
- [75] R. A. Kendall, T. H. Dunning, and R. J. Harrison, Electron affinities of the first-row atoms revisited. systematic basis sets and wave functions, *The Journal of chemical physics* **96**, 6796 (1992).